

TORC1 Regulates Endocytosis via Npr1-Mediated Phosphoinhibition of a Ubiquitin Ligase Adaptor

Jason A. MacGurn,^{1,2} Pi-Chiang Hsu,^{1,2} Marcus B. Smolka,¹ and Scott D. Emr^{1,*}

¹Weill Institute for Cell and Molecular Biology, Department of Molecular Biology and Genetics, Cornell University, Ithaca, NY 14853, USA

²These authors contributed equally to this work

*Correspondence: sde26@cornell.edu

DOI 10.1016/j.cell.2011.09.054

SUMMARY

The TORC1 kinase signaling complex is a key determinant of cell growth that senses nutritional status and responds by coordinating diverse cellular processes including transcription, translation, and autophagy. Here, we demonstrate that TORC1 modulates the composition of plasma membrane (PM) proteins by regulating ubiquitin-mediated endocytosis. The mechanism involves the Npr1 kinase, a negative regulator of endocytosis that is itself negatively regulated by TORC1. We show that Npr1 inhibits the activity of Art1, an arrestin-like adaptor protein that promotes endocytosis by targeting the Rsp5 ubiquitin ligase to specific PM cargoes. Npr1 antagonizes Art1-mediated endocytosis via N-terminal phosphorylation, a modification that prevents Art1 association with the PM. Thus, our study adds ubiquitin ligase targeting and control of endocytosis to the known effector mechanisms of TORC1, underscoring how TORC1 coordinates ubiquitin-mediated endocytosis with protein synthesis and autophagy in order to regulate cell growth.

INTRODUCTION

Decisions of cell growth and differentiation are made by complex signaling networks that integrate various environmental and nutritional inputs and respond by coordinating diverse cellular processes toward a specific outcome. One example involves the target of rapamycin complex 1, or TORC1, a highly conserved multiprotein kinase complex that senses various cellular and environmental cues including nutrient availability, energy status, and growth signals and responds by coordinating activities associated with cell growth and proliferation. In general, signals that promote TORC1 kinase activity also promote cell growth and proliferation, whereas signals that inhibit TORC1 kinase activity tend to induce a starvation response. For example, TORC1 kinase phosphorylates both ribosomal S6 kinases and inhibitory eIF4E binding proteins, activities that promote translation initiation (Holz et al., 2005). The TORC1

kinase also phosphorylates Atg13, preventing its association with Atg1 and thereby inhibiting the initiation of autophagy (Kamada et al., 2010), a conserved protein degradation pathway crucial to the starvation response in eukaryotic cells. Thus, TORC1 signaling coordinates cell growth by simultaneously promoting protein synthesis and inhibiting autophagy, whereas loss of TORC1 signaling triggers the onset of the starvation response by decreasing protein synthesis and inducing autophagy.

Some of the factors that regulate TORC1 signaling have been studied in detail. One important upstream activator of TORC1 signaling is Rheb, a lysosome-localized small GTPase that is antagonized by the GAP activity of TSC1-TSC2 heterodimers (Inoki et al., 2003). TSC2 is a key point of signal integration for TORC1 signaling: growth factors can stimulate TORC1 signaling via Akt/PKB-mediated inhibition of TSC2 (Inoki et al., 2002; Manning et al., 2002), whereas energy starvation can inhibit TORC1 signaling via AMPK-dependent phosphoactivation of TSC2 (Inoki et al., 2003). TORC1 signaling also responds to protein misfolding and quality control by sensing the availability of molecular chaperones, allowing the cell to regulate growth in response to protein folding stress (Qian et al., 2010). Via mechanisms that are not completely understood, TORC1 also senses and responds to amino acid availability. This mode of TORC1 regulation involves the activity of four Rag GTPases that regulate amino acid-dependent localization of TORC1 to the lysosome, thus promoting interaction with and activation by Rheb (Sancak et al., 2010). Despite numerous reports elucidating the nutritional and environmental cues that influence TORC1 signaling and its downstream effector responses, a mechanistic understanding of how TORC1 integrates multiple signals to coordinate a holistic growth strategy for the cell remains to be elucidated.

Another way that eukaryotic cells regulate growth and proliferation in response to environmental changes is by regulating the activity and abundance of specific proteins at the cell surface. This is largely achieved via endocytic downregulation, which involves the endocytosis of cell surface proteins followed by delivery to the lysosome (or vacuole) where degradation occurs. Such endocytic downregulation is critical to human health and disease. For example, failure to attenuate growth factor signaling from ligand-bound EGF receptor by endocytic downregulation can result in the aberrant proliferation of cells and cause cancer. To prevent hyperproliferation, the ubiquitin ligase Cbl and the adaptor protein Grb2 mediate the ubiquitination of stimulated

EGFR molecules at the cell surface, targeting them for endocytosis and subsequent lysosomal degradation (Miranda and Sorkin, 2007). This example highlights the key role that endocytic downregulation plays in growth signal attenuation. While endocytic downregulation has been extensively studied as a mechanism for attenuation of signaling processes, less is known about how cells regulate surface protein abundance in response to changes in nutrient availability or cellular stress. Understanding how cells regulate the abundance and activity of cell surface proteins in response to changes in environment and nutrient availability is key to deciphering cellular strategies for adaptive growth.

In this study, we report that TORC1 signaling controls nutrient uptake by targeting the ubiquitin-mediated endocytosis of specific amino acid transporters. The mechanism involves a negative kinase signaling cascade in which TORC1 kinase inhibits the nitrogen permease reactivator 1 (Npr1) kinase, which in turn inhibits a ubiquitin ligase adaptor. This ubiquitin ligase adaptor, the arrestin-related protein Art1, was previously shown to recruit Rsp5, the yeast homolog of Nedd4, to specific proteins at the plasma membrane (PM) in order to target them for endocytosis (Lin et al., 2008). We show that the TORC1-Npr1 negative kinase signaling cascade regulates Art1 translocation to the PM by N-terminal phosphorylation. Our results demonstrate that a key effector pathway of TORC1 signaling coordinates the targeting of a ubiquitin ligase in order to regulate the endocytosis and vacuolar trafficking of specific nutrient transporters at the plasma membrane. Furthermore, these findings reveal that TORC1 controls amino acid uptake by tuning the abundance of transporters at the cell surface and that coordination of endocytosis with other cellular processes such as transcription, translation, and autophagy is critical for the ability of cells to adapt to changes in nutrient availability.

RESULTS

TORC1 Regulates Endocytosis of Amino Acid Transporters

Previously we demonstrated that treatment of yeast cells with cycloheximide triggers the endocytosis and vacuolar trafficking of various plasma membrane proteins (Lin et al., 2008). We hypothesized that this might be part of a global cellular response to changes in nutrient availability, especially considering that cycloheximide has been shown to hyperactivate TORC1 signaling (Binda et al., 2009). We decided to test whether TORC1 signaling regulates the endocytosis, trafficking, or activity of cell surface proteins. First, we took advantage of the toxic arginine analog canavanine, which enters the cell through the arginine transporter Can1. Thus, sensitivity to canavanine is a function of the PM localization and activity of Can1. Previously, we used canavanine sensitivity to identify mutant strains defective for Can1 endocytosis (Lin et al., 2008). We observed that cells deleted for *TCO89*, a subunit of the yeast TORC1 signaling complex, exhibited canavanine hypersensitivity (Figure 1A) consistent with a potential defect in endocytosis. In contrast, mutants defective for TORC2, a related but distinct signaling complex that controls cell growth, survival and polarization, did not exhibit canavanine hypersensitivity (Figure 1A). These results

suggested that TORC1 signaling may play a role in the endocytosis or the activity of Can1 at the cell surface.

To determine if TORC1 signaling is required for cycloheximide-triggered endocytosis, we examined Can1-GFP vacuolar trafficking in wild-type yeast cells treated with either cycloheximide or cycloheximide and rapamycin, a potent TORC1 inhibitor. Interestingly, rapamycin inhibited the endocytosis and vacuolar trafficking of Can1-GFP in cycloheximide-treated cells (Figure 1B), suggesting a role for TORC1 in the endocytosis of Can1. Consistent with these results, we found that treatment of yeast cells with cycloheximide dramatically reduced arginine uptake, while simultaneous treatment with rapamycin abrogated this affect (Figure 1C). These results demonstrate that TORC1 signaling promotes the endocytic downregulation of the arginine transporter Can1.

Since many PM proteins undergo endocytosis and vacuolar trafficking in response to cycloheximide treatment, we tested additional cargo proteins and found that the cycloheximide-triggered endocytosis of the uracil transporter Fur4 and the methionine transporter Mup1 was abrogated in the presence of rapamycin (Figure 1D and Figure S1 (available online), respectively). Interestingly, rapamycin treatment did not affect the uracil-induced endocytosis of Fur4 (Figure 1D) or the methionine-induced endocytosis of Mup1 (Figure S1), indicating that TORC1 signaling is not required for substrate-triggered endocytosis. Instead, these results suggest that TORC1 signaling promotes the endocytosis of multiple cell surface proteins as a general mechanism to limit protein abundance at the PM. Given our previous findings that cycloheximide-induced endocytosis of Can1 depends on the arrestin-like adaptor protein Art1 (Lin et al., 2008), which targets the Rsp5 ubiquitin ligase to specific cargoes at the PM, we hypothesized that TORC1 control of ubiquitin-mediated endocytosis may occur via regulation of Art1 function (Figure 1E). We set out to elucidate the molecular mechanisms that govern TORC1-mediated endocytosis.

The TORC1 Effector Kinase Npr1 Negatively Regulates Endocytosis

To determine how TORC1 regulates endocytosis, we scored the canavanine growth phenotypes of yeast deletion strains lacking different candidate effector kinases downstream of TORC1. We hypothesized that yeast cells deleted for TORC1-activated effector pathways that mediate Can1 endocytosis would exhibit hypersensitivity to canavanine. Although we did not observe any significant canavanine hypersensitive phenotypes among these deletion strains (Figure 2A, middle panel), we did observe a striking canavanine resistance phenotype in $\Delta npr1$ cells (Figure 2A, right panel). Npr1 is a protein kinase known to be phosphorylated and inhibited in a TORC1-dependent manner by a mechanism that likely involves both direct phosphorylation (Breitkreutz et al., 2010) and indirect control by regulation of a phosphatase that dephosphorylates and activates Npr1 (Figure S2A) (Bonenfant et al., 2003). We found that complementation of the canavanine resistance phenotype of $\Delta npr1$ cells required the Npr1 kinase activity (Figure 2B), suggesting that the Npr1 kinase negatively regulates Can1 endocytosis. We also observed that the canavanine resistance phenotype in $\Delta npr1$ cells required intact endocytic machinery (Figure S2B),

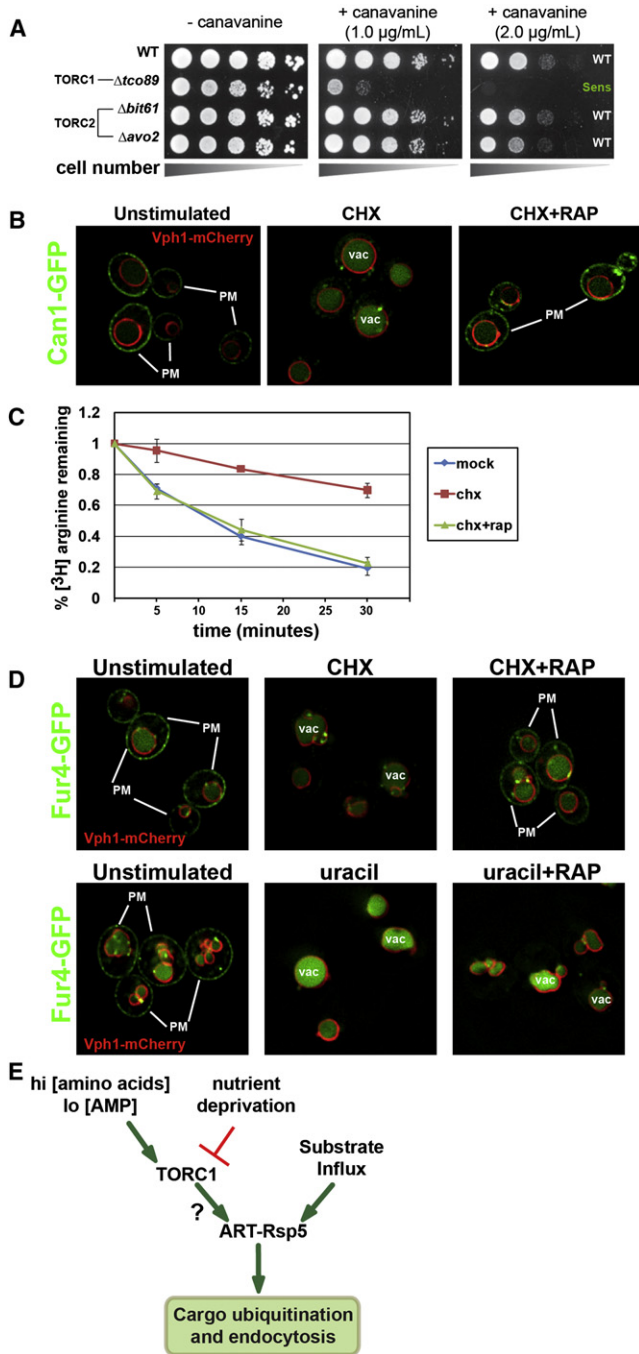


Figure 1. TORC1 Regulates the Endocytosis of Amino Acid Transporters

(A) Wild-type (background BY4741), TORC1-, and TORC2-deficient yeast cells from the yeast deletion strain collection were scored for growth in the presence of canavanine.

(B) Fluorescence distribution of Can1-GFP (green) was analyzed in wild-type yeast cells expressing the vacuolar marker Vph1-mCherry (red). Cells were either mock-treated (unstimulated) or treated with cycloheximide (CHX) or cycloheximide and rapamycin (CHX+RAP) for 4 hr. Plasma membrane (PM) and vacuole (vac) localization are indicated.

(C) The uptake of [³H]arginine was measured in cells that were mock treated (blue), cycloheximide treated (red), or treated with cycloheximide and rapa-

mycin (green). Error bars indicate standard deviation calculated from three replicate experiments. (D) Fluorescence distribution of Fur4-GFP (green) was analyzed in wild-type yeast cells expressing the vacuolar marker Vph1-mCherry (red). The affect of the following treatments were analyzed: mock-treated (unstimulated), cycloheximide-treated (CHX), cycloheximide- and rapamycin-treated (CHX+RAP), uracil-treated (URA), uracil- and rapamycin-treated (URA+RAP). All cells were imaged after 60 min of treatment. (E) TORC1-regulated endocytosis may be mediated via the regulation of ART-Rsp5 ubiquitin ligase complexes. See also Figure S1.

suggesting that this phenotype is linked to endocytosis and not a Golgi-to-endosome shunt. To explore this further, we examined the steady state localization of Can1-GFP in wild-type and $\Delta npr1$ cells and found that deletion of the Npr1 kinase resulted in constitutive endocytosis and vacuolar trafficking of Can1-GFP (Figure 2C). Additional analysis revealed a similar role for Npr1 in the negative regulation of Fur4 and Lyp1 endocytosis (Figures S2C–S2E), whereas Mup1-GFP was unaffected in $\Delta npr1$ cells (Figure S2F). Npr1-related kinases such as Hrk1 (26.4% identical) and Prr2 (34.5% identical) do not exhibit growth phenotypes in the presence of canavanine (Figure S2G), highlighting the specialized role of Npr1 as a negative regulator of endocytosis. To confirm the relationship between Npr1 and TORC1 kinases, we analyzed the canavanine growth phenotype of $\Delta tco89 \Delta npr1$ double-mutant cells and determined that they exhibited a canavanine resistance similar to $\Delta npr1$ cells (Figure 2D). The observation that canavanine hypersensitivity of $\Delta tco89$ cells is dependent on the presence of Npr1 indicates that TORC1 controls endocytosis via negative regulation of the Npr1 kinase. To confirm that Npr1 activity negatively regulates endocytosis, we analyzed the affect of titrating Npr1 expression in wild-type yeast cells. We found that increased expression of the Npr1 kinase translated to a corresponding increase in canavanine sensitivity (Figure 2E), demonstrating that increased levels of Npr1 protein result in hyper-stabilization of Can1 at the plasma membrane.

Npr1 Regulates Art1 Activity via Phosphoinhibition

To decipher the mechanism by which Npr1 negatively regulates endocytosis, we used stable isotope labeling of amino acids in culture (SILAC) followed by phosphopeptide enrichment and quantitative mass spectrometry analysis to identify candidate substrates of the Npr1 kinase in an unbiased fashion. Since rapamycin is known to stimulate Npr1 kinase activity via inhibition of TORC1 (Gander et al., 2008), we compared the phosphoproteome of wild-type yeast cells treated with rapamycin to that of $\Delta npr1$ cells treated with rapamycin in order to identify modifications that are dependent on Npr1 kinase activity (Table 1). Using this approach, we identified several candidate Npr1 substrates including several proteins with established roles in membrane traffic and nutrient transport. One of the candidates identified by this approach was Art1, which is required for cycloheximide-induced ubiquitination and endocytosis of Can1 (Figure 1E) (Lin et al., 2008). The identification of Art1 as a candidate substrate of Npr1 suggested that Npr1 may negatively regulate endocytosis via phosphoregulation of Art1. Genetic interaction analysis revealed that the canavanine resistance phenotype of

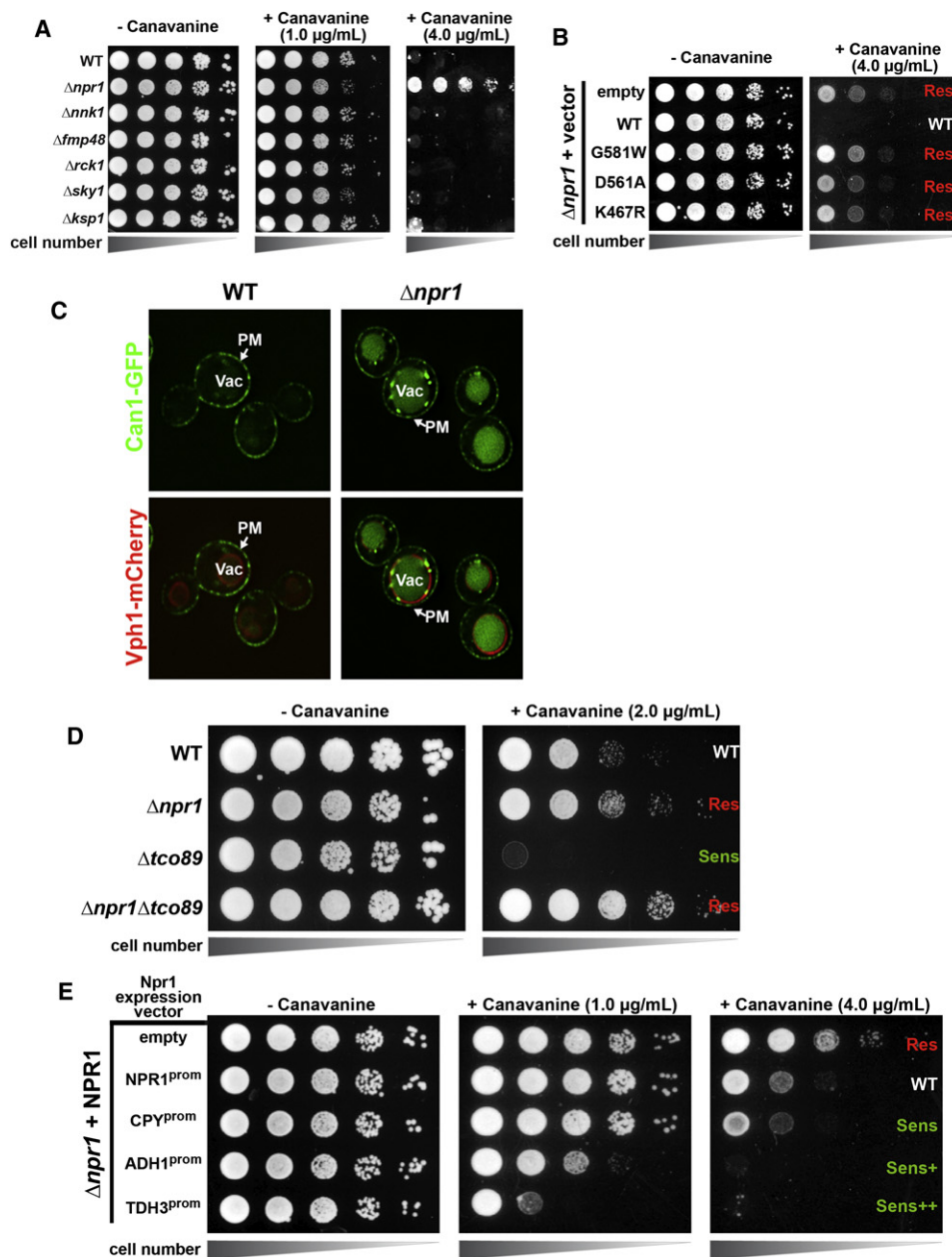


Figure 2. The TORC1 Effector Npr1 Negatively Regulates Endocytosis

(A) Wild-type (background BY4741) yeast cells and yeast cells defective for effector pathways downstream of TORC1 were scored for growth in the presence of canavanine.

(B) Complementation of the canavanine resistance phenotype exhibited by $\Delta npr1$ yeast cells was tested using vectors expressing *NPR1* alleles under the control of its native promoter. Tested alleles included wild-type (WT) *NPR1*, a kinase activation loop mutant (*npr1-G581W*), a catalytic site mutant (*npr1-D561A*), and an ATP-binding pocket mutant (*npr1-K467R*).

(C) Fluorescence microscopy analysis of Can1-GFP (green) in unstimulated wild-type and $\Delta npr1$ yeast cells. Vph1-mCherry (red) was used to label vacuoles. Plasma membrane (PM) and vacuole (Vac) are indicated.

(D) Growth of wild-type (BY4741), $\Delta npr1$, $\Delta tco89$, and $\Delta npr1\Delta tco89$ yeast cells in the presence of canavanine was compared.

(E) Expression of wild-type Npr1 was titrated using the following series of promoters: pNpr1 (endogenous), pCPY, pADH, and pTDH3. The affects of Npr1 titration on Can1 trafficking were determined by assaying growth in the presence of canavanine.

See also Figure S2.

Table 1. The Npr1 Phosphoproteome Reveals Art1 as a Downstream Effector

Category	Protein	Description	Xpress Ratios
Control	Npr1	Protein Kinase	107
Trafficking	Art1	Rsp5 ubiquitin ligase adaptor	27, 11
	SEC7	Arf GEF	27, 24
	TRS120	TRAPP complex component	121, 60
	LSP1	Eisosome component	79
Integral membrane proteins and transporters	VCX1	ion antiporter	117, 46, 17
	AGP1	amino acid transporter	98
	ITR1	inositol transporter	10
	GNP1	amino acid transporter	21, 10
Actin and polarization	RHO1	GTPase	215
	BEM3	RhoGAP	12
Lipid synthesis and binding	NUS1	prenyltransferase	10
	PIB2	PI3P binding protein	36
	ORM1	lipid homeostasis	39, 28, 12
Metabolic enzymes	IPP1	pyrophosphatase	88
Mito. import	TOM22	mitochondrial protein import	27
Function unknown	YLR257W	function unknown	62, 46, 32, 12

Wild-type cells (labeled with heavy isotopes) and $\Delta npr1$ cells (labeled with light isotopes) were treated with rapamycin for 15 min and the phosphoproteome of each was quantitatively assessed using SILAC. A total of 3,652 phosphopeptides were identified in this experiment. Xpress ratio indicates the fold enrichment in wild-type cells compared to $\Delta npr1$ cells. This table shows proteins containing phosphopeptides that exhibited at least a 10-fold increase in wild-type cells relative to $\Delta npr1$ cells.

$\Delta npr1$ cells is dependent upon the presence of Art1 (Figure 3A), suggesting that Npr1 negatively regulates endocytosis via inhibition of Art1. Furthermore, the constitutive endocytosis and vacuolar trafficking of Can1-GFP observed in $\Delta npr1$ cells was suppressed in $\Delta npr1 \Delta art1$ double-mutant cells (Figures 3B and 3C), indicating that the aberrant endocytosis of Can1-GFP observed in $\Delta npr1$ cells is mediated by Art1.

Based on these results, we hypothesized that the TORC1-Npr1 negative kinase signaling cascade regulates Art1 activation by phosphoinhibition (Figure 3D). A key prediction of this hypothesis is that loss of Npr1 kinase activity would alter the phosphorylation status of the Art1 protein. Consistent with this hypothesis, we found that Art1 recovered from $\Delta npr1$ cells exhibited a >50% decrease in the amount of phosphate incorporation relative to wild-type cells (Figure 3E). Furthermore, we found that the Art1 protein recovered from wild-type cells exists in two distinct forms, resolved as a doublet by SDS-PAGE (Figure 3F, lane 1). Following phosphatase treatment, the Art1 doublet collapses to a single band (Figure 3F, lane 2), indicating that the lower mobility form of Art1 is phosphorylated. Interestingly, Art1

protein recovered from $\Delta npr1$ cells did not exhibit the phosphoshift observed in wild-type cells (Figure 3F, lanes 3 and 4). Art1 phosphorylation was complemented by expression of wild-type Npr1 but not kinase-dead mutant alleles (Figure 3G). Furthermore, increasing Npr1 expression led to corresponding increases in Art1 phosphorylation (Figure 3H and Figure S3). Finally, we were able to demonstrate that Art1 is a substrate for active Npr1 kinase but not a kinase dead mutant in vitro (Figure 3I), providing evidence for direct phosphorylation. In summary, these results suggest that Npr1 negatively regulates endocytosis by phosphorylating Art1, a ubiquitin ligase adaptor.

TORC1 Signaling Tunes Art1 Activity by Modulating Phosphoinhibition

To test whether TORC1 activity mediates Art1 dephosphorylation, we examined radioactive phosphate incorporation into Art1 under conditions of TORC1 hyperactivation. We found that hyperactivation of TORC1 signaling by treatment of yeast cells with cycloheximide resulted in a >60% decrease in Art1 phosphorylation (Figure 4A). Based on our data, we propose a TORC1-Npr1 negative kinase signaling cascade that activates Art1 via sequential repression (Figure 4B). In this model, inhibition of TORC1 signaling (by starvation conditions or treatment of cells with rapamycin) triggers Npr1 activation by dephosphorylation. The increased Npr1 kinase activity leads to inhibition of Art1, which decreases endocytosis and stabilizes Can1 at the PM (Figure 4C lane 1, Figure 4D, and Figure S4A). When TORC1 activity is high (in nutrient-replete conditions or by treatment of cells with cycloheximide), Npr1 is hyperphosphorylated and its kinase activity is inhibited. This state favors Art1 dephosphorylation, which leads to increased Can1 endocytosis and vacuolar degradation (Figure 4C, lane 3, Figure 4D, and Figure S4A). During normal log phase growth conditions, TORC1 signals at an intermediate level, maintaining both Art1 and Npr1 in a metaphosphorylated state (Figure 4C, lane 2, Figure 4D, and Figure S4A). This system endows TORC1 with fine control over the endocytic equilibrium of Can1, effectively tuning nutrient transport over a wide range of conditions. This signaling pathway responds to perturbations in TORC1 signaling within minutes (Figures S4B and S4C, and unpublished data), and the response to both cycloheximide and rapamycin is dependent on TORC1 but not TORC2 (data not shown). Consistent with these results, the ability of cycloheximide to activate Art1 by inhibiting Npr1 is blocked by simultaneous treatment with rapamycin (Figure 4E). We also found that regulation of Can1 endocytosis by TORC1 translates to corresponding effects on arginine uptake: TORC1 signaling increased Can1 endocytosis and thus blocked arginine uptake, while TORC1 inhibition stabilized Can1 at the PM and thus increased the rate of arginine uptake (Figure S4D). These data support a model whereby TORC1 regulates endocytosis via a negative kinase cascade that tunes Art1 activity by phosphoinhibition.

To further explore the basis for TORC1 regulation of endocytosis, we examined Art1 phosphorylation across a variety of media conditions and cellular stresses. Similar to our results with rapamycin treatment, we found that shifting from minimal media to PBS, a physiological starvation condition, triggered

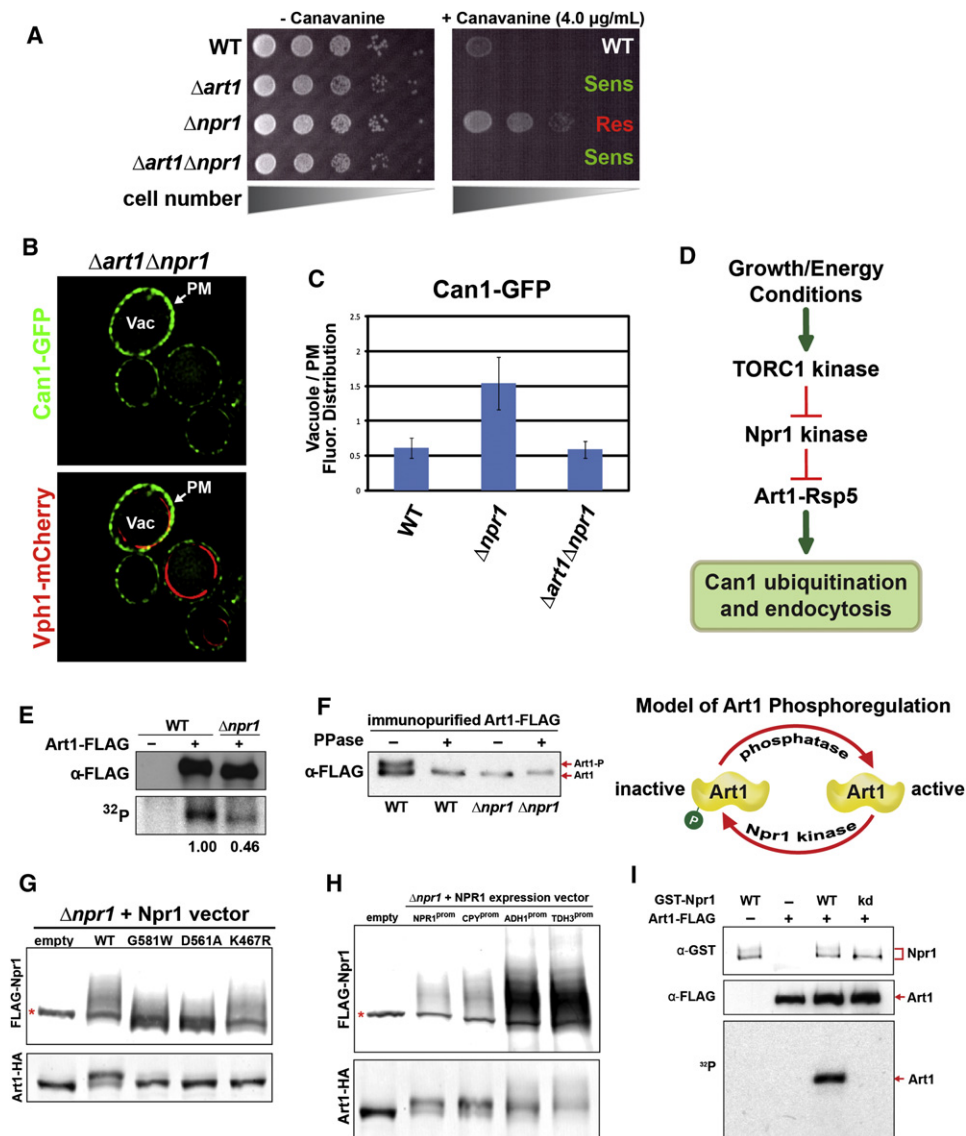


Figure 3. Npr1 Regulates Art1 Activity via Phosphoinhibition

- (A) Canavanine sensitivity/resistance phenotypes were determined for wild-type (WT), $\Delta art1$, $\Delta npr1$, $\Delta art1\Delta npr1$ cells.
- (B) Fluorescence microscopy analysis of Can1-GFP (green) in unstimulated $\Delta art1\Delta npr1$ yeast cells. Vph1-mCherry (red) was used to label vacuoles.
- (C) Quantitative analysis of Can1-GFP distribution in cells from (B) and Figure 2C. Fluorescence intensity of PM and vacuole was averaged over a population of cells ($n > 50$) for each genotype.
- (D) Based on genetic interaction data, we devised a model pathway for the TORC1-Npr1 negative signaling cascade that results in phosphoregulation of Art1. This pathway controls the cycling of Art1 between a phosphorylated inactive state and a dephosphorylated active state.
- (E) Art1 was affinity purified from unstimulated wild-type and $\Delta npr1$ yeast cells labeled with ^{32}P . Top panel depicts western blot of total Art1 protein recovered, while bottom panel shows ^{32}P incorporation into Art1. Quantitation was performed by scanning Phosphorimager (bottom labels).
- (F) Art1 was affinity purified from wild-type or $\Delta npr1$ yeast cells and subject to phosphatase treatment or mock treatment. Affinity-purified Art1 from wild-type cells can be resolved as two distinct bands, indicated by red arrows on the right.
- (G) Western blot analysis of Npr1 expression levels (top panel) and Art1 phosphorylation patterns (bottom panel) for complementation vectors in Figure 2B. Red asterisk indicates a nonspecific band.
- (H) Expression of wild-type Npr1 was titrated using same parameters as in Figure 2E. Npr1 expression (top panel) and Art1 phosphorylation patterns (bottom panel) were analyzed by western blot. See also Figure S3.
- (I) Phosphorylation of recombinant Art1 was reconstituted using wild-type (WT) but not kinase dead (kd) Npr1 purified from yeast.

Art1 hyperphosphorylation (Figure 4F, lane 3). In contrast, shifting yeast cells from minimal media to nutrient rich YPD triggered Art1 dephosphorylation (Figure 4F, lane 2). Interestingly, Art1

phosphostatus was not sensitive to other cellular stresses tested (Figure 4G). In summary, our results indicate that TORC1 senses nutrient availability and responds by regulating endocytosis in

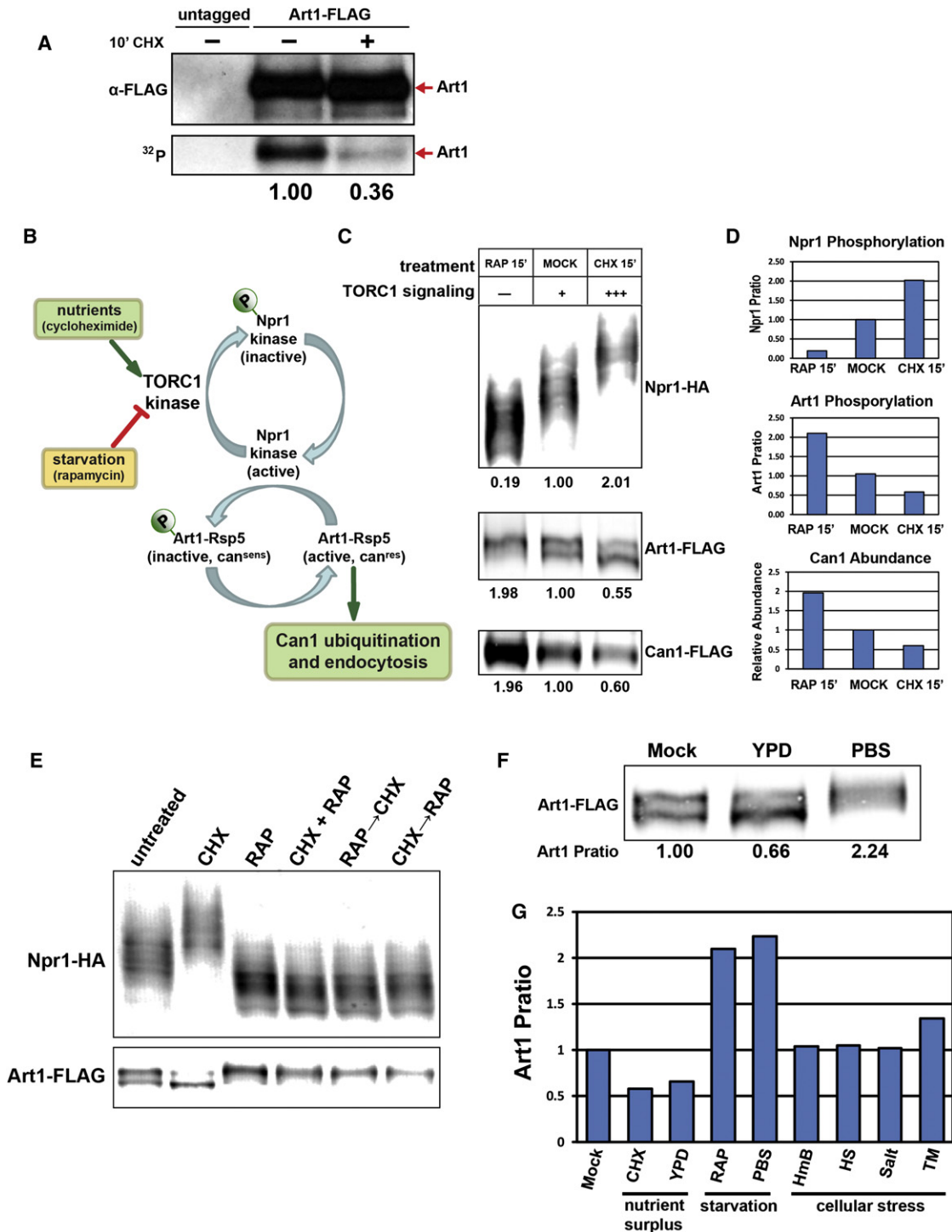


Figure 4. TORC1 Tunes Art1 Activity by Modulating Phosphorylation

(A) Art1 recovered from wild-type yeast cells labeled with 32 P and subject to cycloheximide stimulation or mock treatment. Top panel depicts western blot of total Art1 protein recovered, while bottom panel shows 32 P incorporation into Art1. Quantitation was performed by scanning Phosphorimager (bottom labels).

(B) Model for TORC1 activation of Art1-mediated endocytosis of Can1 by a sequential repression mechanism.

(C) Wild-type yeast cells were treated with rapamycin (200 ng/ml), cycloheximide (50 μ g/ml), or mock-treated (DMSO) for 15 min and analyzed for Npr1 phosphoshift (top panel), Art1 phosphoshift (middle panel), and Can1 abundance (lower panel). Values indicate Npr1 Pratio (below top panel), Art1 Pratio (below middle panel), and Can1 relative abundance (below bottom panel) all normalized to the mock condition. Indicators of TORC1 signaling activity (-, +, +++) are based on previous reports that RAP inhibits TORC1 signaling and CHX activates TORC1 signaling, both relative to mock treatment.

order to tune the activity of amino acid transporters at the cell surface.

Inhibition of Art1 Is Mediated by N-Terminal Phosphorylation

To better understand the mechanism of Art1 phosphoinhibition, we employed quantitative mass spectrometry methodologies to map specific phosphosites in Art1 that are dependent on the TORC1-Npr1 negative kinase signaling cascade. First, we trypsin-digested affinity-purified Art1 from wild-type cells, enriched for phosphopeptides using immobilized metal affinity chromatography (IMAC), and analyzed samples using LC-MS/MS. This analysis revealed many phosphorylated residues in Art1, including an N-terminal phosphocluster (between amino acids 79 and 124), a series of mostly proline-directed phosphosites at the C terminus of Art1 (from amino acids 599 to 722), and a few phosphosites in the arrestin fold domain (Figure 5A). Next, we used SILAC to determine which sites were dependent on Npr1 activity (Figure 5B). We found that both the N-terminal phosphocluster and the proline-directed phosphocluster were dependent on the presence of Npr1 (Figure 5C). Similarly, both clusters increased significantly during rapamycin-induced Art1 hyperphosphorylation (Figure 5D). Interestingly, when we compared Art1 phosphopeptides from rapamycin-treated wild-type cells (hyperphosphorylated) and rapamycin-treated $\Delta npr1$ cells (hypo-phosphorylated), we observed a dramatic 30- to 60-fold difference in phosphorylation at the N-terminal phosphocluster and only modest (4- to 10-fold) increases for the proline-directed phosphocluster (Figure 5E). Furthermore, we found that overexpression of wild-type Npr1 resulted in similarly dramatic increases in phosphorylation at the N-terminal sites compared to overexpression of a kinase-dead variant (Figure 5F). Our quantitative mass spectrometry data strongly suggests that Npr1 promotes phosphorylation at the N terminus of Art1 (especially Ser79, Ser82, Ser96, and Ser99). Our results suggest that Npr1 indirectly affects phosphorylation at C-terminal proline-directed sites in Art1 as previous studies have shown that a +1 proline is strongly disfavored by the Npr1 kinase (Gander et al., 2009), making these sites unlikely targets for direct regulation by Npr1. Indeed, using the in vitro kinase assay, Npr1 was capable of phosphorylating an N-terminal fragment of Art1, but not a C-terminal fragment that contains the proline-directed phosphorylation sites (Figures S5A and S5B). Importantly, we found that the Art1 bandshift observed by SDS-PAGE is dependent on the C-terminal proline-directed phosphorylation events, indicating it is the result of both Npr1 and yet another kinase (Figure S5C). Although in vitro phosphorylation of Art1 by Npr1 did not reconstitute the bandshift observed in vivo (Figure 3I), mass spectrometry analysis of Art1 phosphorylated by Npr1 in vitro identified the same N-terminal phosphorylation pattern (particularly at S79, data not

shown) observed in vivo. Since Art1 C-terminal proline-directed phosphorylation events are in fact regulated by Npr1 in vivo (Figures 5C–5E), our results suggest a possible interaction between N-terminal and C-terminal phosphorylation events, and further investigation will be required to determine the function of proline-directed phosphorylation at the C terminus of Art1.

TORC1-dependent phosphoregulation of other ART family proteins was not evident by SDS-PAGE (Figure S5D), however quantitative mass spectrometry analysis revealed that other ART family proteins, most notably Art2 and Art3, may also be regulated by Npr1 (Figure S5E). These results suggest that TORC1 signaling does not regulate all ART family proteins, but rather appears to specifically regulate Art1 as well as perhaps Art2 and Art3. We also performed similar quantitative mass spectrometry analysis of Npr1 phosphorylation in response to changes in TORC1 signaling. We identified numerous Npr1 phosphosites primarily clustered at the N terminus of the protein (Figure S6A). Consistent with our observations in Figure 4, this N-terminal phosphorylation of Npr1 is significantly reduced when TORC1 is inhibited (Figure S6B) and significantly increased when TORC1 is hyperactivated (Figure S6C). These results are consistent with previously reported mass spectrometry analysis of Npr1 phosphorylation (Gander et al., 2008). Given the large number of N-terminal phosphorylation events that respond in this manner, we deleted the N-terminal phosphocluster of Npr1 ($\Delta 40$ -360) and found that the truncated protein does not complement canavanine resistance or Art1 phosphorylation (Figures S6D and S6E). These results indicate that Npr1 undergoes N-terminal phosphoinhibition similar to Art1 but that this N-terminal region is essential for Npr1-mediated regulation of endocytosis.

To address the function of the Art1 N-terminal phosphocluster, we analyzed the effect of alanine (phosphodead) or aspartic acid (phosphomimetic) substitutions at these residues. Interestingly, we found that no single site substitution had a significant effect on Art1 function. However, we observed dramatic changes in Art1 function when multiple phosphosites were mutated. For example, multiple alanine substitutions at N-terminal phosphosites of Art1 led to a striking canavanine resistance phenotype (Figure 5G), similar to that observed with $\Delta npr1$ cells. Additionally, multiple aspartic acid substitutions at N-terminal phosphosites resulted in canavanine hypersensitivity (Figure 5H), indicating Art1 is stuck in an inhibited, phosphomimetic state. These results indicate that (1) Npr1 mediates the phosphorylation of a distinct cluster of residues at the N terminus of Art1, (2) phosphorylation of these N-terminal residues inhibits Art1-mediated Can1 endocytosis, and (3) dephosphorylation of these residues results in activation of Art1-mediated Can1 endocytosis. Thus, the N-terminal phosphocluster of Art1 is a critical feature of the regulated endocytosis of Can1.

(D) Quantitation of data in (C) using fluorescence scanning as demonstrated in Figure S4A.

(E) The signaling response from (C) was analyzed in response to either cotreatment with or different orders of addition of cycloheximide and rapamycin.

(F) The phosphostatus of Art1 was analyzed in response to changes nutrient availability, including a shift from minimal media to YPD for 2 hr (nutrient surplus) or a shift from minimal media to PBS for 12 hr (starvation).

(G) Quantitation of the Art1 phosphorylation ratio (Pratio) for the results in (F) along with additional treatments including 200 μ g/ml Hygromycin B for 15 min (HmB), heat shock at 37° for 30 min (HS), 0.4M NaCl for 30 min (salt), or 4 μ g/ml tunicamycin for 15 min (TM).

See also Figure S4.

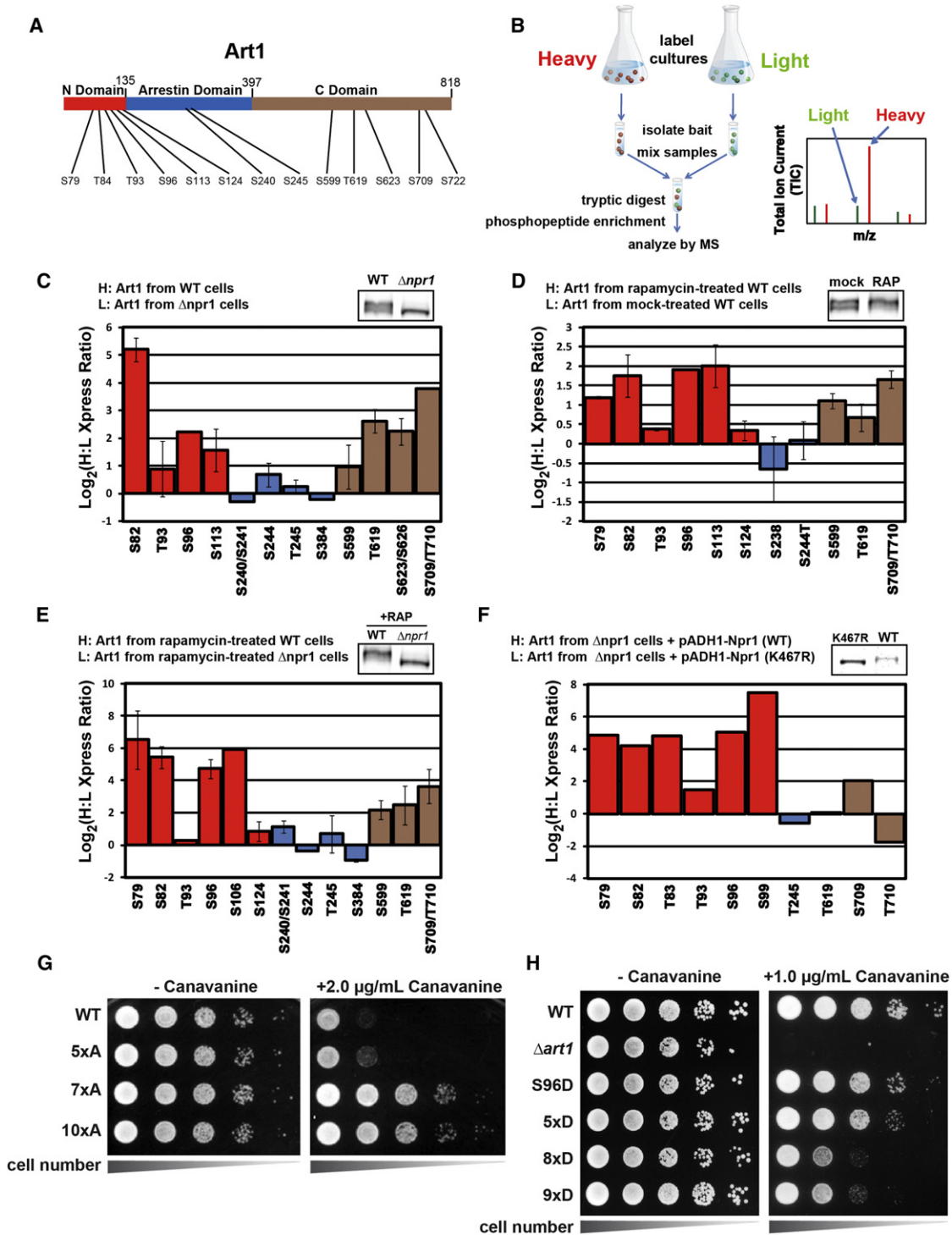


Figure 5. Inhibition of Art1 Is Mediated by N-Terminal Phosphorylation

(A) Schematic dividing the Art1 protein into three regions: an N-terminal domain (red), the arrestin fold domain (blue), and a C-terminal domain (brown). Phosphorylation sites identified by mass spectrometry analysis are indicated. (B) Schematic demonstrating how SILAC followed by quantitative mass spectrometry analysis is used to measure changes at specific Art1 phosphosites. SILAC combined with quantitative mass spectrometry analysis was used to measure changes in phosphorylation at specific Art1 residues for pair wise comparisons of wild-type (WT) cells versus $\Delta npr1$ cells (C), rapamycin-treated WT cells versus mock-treated WT cells (D), rapamycin-treated WT cells versus rapamycin-treated $\Delta npr1$ cells (E), and $\Delta npr1$ cells overexpressing WT Npr1 versus $\Delta npr1$ cells overexpressing the kinase dead *npr1-K467R* allele (F). For each of C-F, bars are color-coded to reflect the position of the phosphosites in the Art1 protein (as indicated in [B]). The y axis values represent the Log_2 of the Xpress (H:L) ratio, a quantitative measure of isotopic representation. Western blots showing

N-Terminal Phosphorylation Antagonizes Art1 PM Recruitment

We next investigated how N-terminal phosphorylation of Art1 inhibits Can1 endocytosis. First, we considered the possibility that N-terminal phosphorylation could lower the affinity of Art1 for Rsp5, however our quantitative mass spectrometry results indicated that changes in Art1 phosphostatus do not affect its interaction with Rsp5 (Figure S7A).

Previously, we showed that GFP-tagged Art1 in unstimulated wild-type cells localizes to the cytosol, Golgi, and plasma membrane (Figure S7B, top panels) and cycloheximide-induced activation of endocytosis results in translocation of Art1 to the PM (Figure 6A, top panels) (Lin et al., 2008). Interestingly, we found that cycloheximide-induced PM recruitment of Art1 was blocked by addition of rapamycin (Figure 6A, bottom panels), and that wild-type cells treated with rapamycin exhibited less Art1-GFP at the plasma membrane compared to untreated cells (Figure S7B, bottom panels). Since these treatments “toggle” Art1 between phosphorylated and dephosphorylated states, the effect of rapamycin and cycloheximide on Art1 localization suggested that N-terminal phosphorylation may regulate Art1 recruitment to the plasma membrane.

To further explore this possibility, we mixed wild-type cells (marked with Sec7-Mars) and $\Delta npr1$ cells both expressing Art1-GFP. We treated this mixed culture with rapamycin, so that Art1 in wild-type cells would be hyperphosphorylated and Art1 in $\Delta npr1$ cells would be hypophosphorylated (Figure 6B, inset). Interestingly, when we analyzed Art1-GFP distribution in the mixed culture, we found that hyperphosphorylated Art1 in the wild-type cells was localized primarily to the cytosol and Golgi, while hypophosphorylated Art1 in the $\Delta npr1$ cells accumulated extensively at the plasma membrane (Figures 6B and 6D). Furthermore, we found that alanine substitution at the N-terminal phosphosites resulted in increased PM recruitment even after treatment of cells with rapamycin (Figures 6C and 6D).

To determine where in the cell Npr1 might phosphorylate Art1, we analyzed the subcellular localization of GFP-Npr1 and found that in unstimulated or cycloheximide-treated cells Npr1 was exclusively cytosolic (Figure 6E, left and middle panels). In contrast, treatment of cells with rapamycin resulted in the PM recruitment of GFP-Npr1 (Figure 6E, right panels, Figure 6F, and Figure S7D). To test the possibility that Art1 and Npr1 interact on the plasma membrane, we performed fluorescence colocalization microscopy using Art1-mCherry and GFP-Npr1. Interestingly, when cells were treated with rapamycin to trigger Npr1 PM recruitment, we observed colocalization of GFP-Npr1 punctae with Art1-mCherry punctae at the plasma membrane (Figure 6G). Although the colocalization we observed was limited, this result is consistent with a transient association of Npr1 with Art1 at the plasma membrane, whereby phosphorylation of Art1 limits its PM association.

DISCUSSION

We have uncovered an effector pathway downstream of TORC1 that regulates the composition of proteins at the PM by controlling endocytosis. Specifically, we show that (1) TORC1 signaling regulates ubiquitin ligase targeting and endocytosis of nutrient transporters at the PM, (2) the effector mechanism that regulates endocytosis involves a TORC1-Npr1 negative kinase signaling cascade that tunes the phosphoinhibition of the ubiquitin ligase adaptor Art1, and (3) the inhibition of Art1 requires phosphorylation at an N-terminal cluster of residues that control Art1 translocation to the PM (Figure 7). These findings establish a unique effector branch of the TORC1 signaling pathway that allows the cell to coordinate the activity of nutrient transporters at the PM as part of a global cellular strategy to regulate cell growth (Figure 7).

A Global Strategy for Regulating Endocytosis

The role of TORC1 as a regulator of ubiquitin-mediated endocytosis is intriguing, because it demonstrates how diverse environmental and nutritional cues such as amino acid availability, energy status, and protein folding stress can affect changes in the abundance of proteins at the cell surface. In contrast to this global mode of TORC1-mediated endocytosis, many well-studied systems of endocytic downregulation involve specific targeting mechanisms, exemplified by the endocytosis-mediated attenuation of activated cell surface receptors such as EGFR and GPCRs in mammalian cells. The results presented in this study demonstrate that nutrient transporters in yeast are subject to both global signals mediated by TORC1 and specific signals that are substrate-dependent. Although these global and specific pathways operate independently in response to distinct cues (Figure 1D and Figure S1), they converge on the same molecular mechanism of control by regulating the function of ubiquitin ligase adaptors (Figure 1E). This sort of signal integration allows TORC1 to bypass specific mechanisms of endocytic downregulation, adding a substrate-independent layer of endocytic control that is sensitive to the growth conditions of the cell.

Proteome-wide analysis of phosphorylation in yeast has demonstrated that ART family proteins are extensively phosphorylated (Albuquerque et al., 2008), and one recent study demonstrated that Npr1 can phosphorylate Art3 in vitro, although the functional significance of this modification remains unclear (O'Donnell et al., 2010). Interestingly, Art3 was recently shown to regulate the ubiquitination and endocytosis of the aspartic acid transporter Dip5 (Hatakeyama et al., 2010). We speculate that Npr1 could negatively regulate the endocytosis of Dip5 via phosphoinhibition of Art3, similar to its role as a negative regulator of Art1. Our phosphoproteomics experiments (Figure S5C) reveal that, while most ART phosphopeptides detected appeared to be Npr1-independent, Npr1-dependent phosphorylation events were detected in Art2 and Art3. Whether or not

phosphoshifts as resolved by SDS-PAGE are shown in the upper right of each profiling experiment. Not all phosphopeptides were detected in every experiment, leading to variation in what can be scored for each condition. Alanine substitution mutant alleles (G) and phosphomimetic substitution alleles (H) of Art1 were analyzed for growth in the presence of canavanine. Labels correspond to the following substitution mutations. 5xA: S79, 82-85A. 7xA: S79, 82-85, 92, 93A. 10xA: S79, 82-85, 92, 93, 96, 99, 100A. 5xD: S79, 82-85D. 8xD: S79, 82-85, 92, 93, 96D. 9xD: S79, 82-85, 92, 93, 96, 113D. See also Figure S5 and Figure S6.

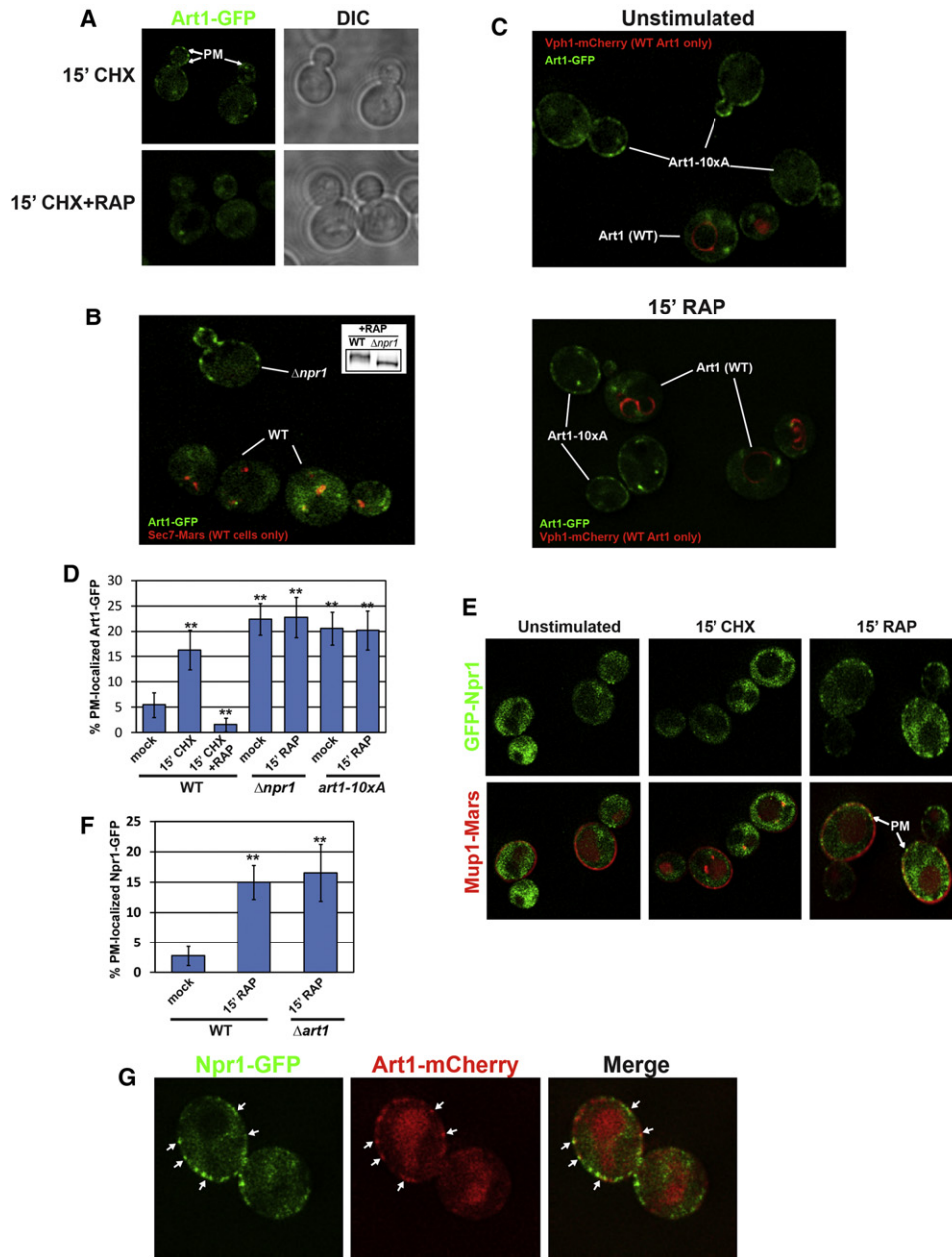


Figure 6. Art1 Phosphorylation Inhibits PM Recruitment

(A) Subcellular localization of Art1-GFP (green) was determined using fluorescence microscopy imaging of wild-type yeast cells. Cells were either treated with cycloheximide (“CHX”) or cotreated with cycloheximide and rapamycin (“CHX+RAP”).

(B) Wild-type yeast cells (labeled with Sec7-Mars (red)) or $\Delta npr1$ cells expressing Art1-GFP were mixed and treated with rapamycin (200 ng/ml for 15 min) and Art1 subcellular localization was analyzed using fluorescence microscopy. The inset is a western blot demonstrating the phosphostatus of Art1 in each condition.

(C) Wild-type yeast cells expressing wild-type Art1-GFP (labeled with Vph1-mCherry (red)) or the N-terminal alanine substitution mutant (art1-8xA) were analyzed by fluorescence microscopy following mock (top panel) or rapamycin (bottom panel) treatment.

(D) Art1-GFP PM localization was quantified as illustrated in Figure S7C (n = 40 cells). Results are normalized to the percent PM localized Art1 from wild-type cells treated with rapamycin, a condition where we do not see Art1 PM recruitment.

(E) GFP-Npr1 (green) subcellular localization was analyzed by fluorescence microscopy following mock, cycloheximide, or rapamycin treatments in wild-type yeast cells expressing Mup1-Mars (red) to label the PM.

(F) Npr1 PM localization was quantified as illustrated in Figure S7C (n = 40 cells). Results are normalized to the percent PM localized Npr1 from wild-type cells treated with cycloheximide, a condition where we do not see Npr1 PM recruitment.

(G) Wild-type yeast cells expressing Npr1-GFP and Art1-mCherry were grown to midlog phase in the presence of methionine and treated with rapamycin (200 ng/ml for 5 min). Both Npr1 and Art1 subcellular localization was determined using fluorescence microscopy imaging. ** indicated p < 0.005.

See also Figure S7.

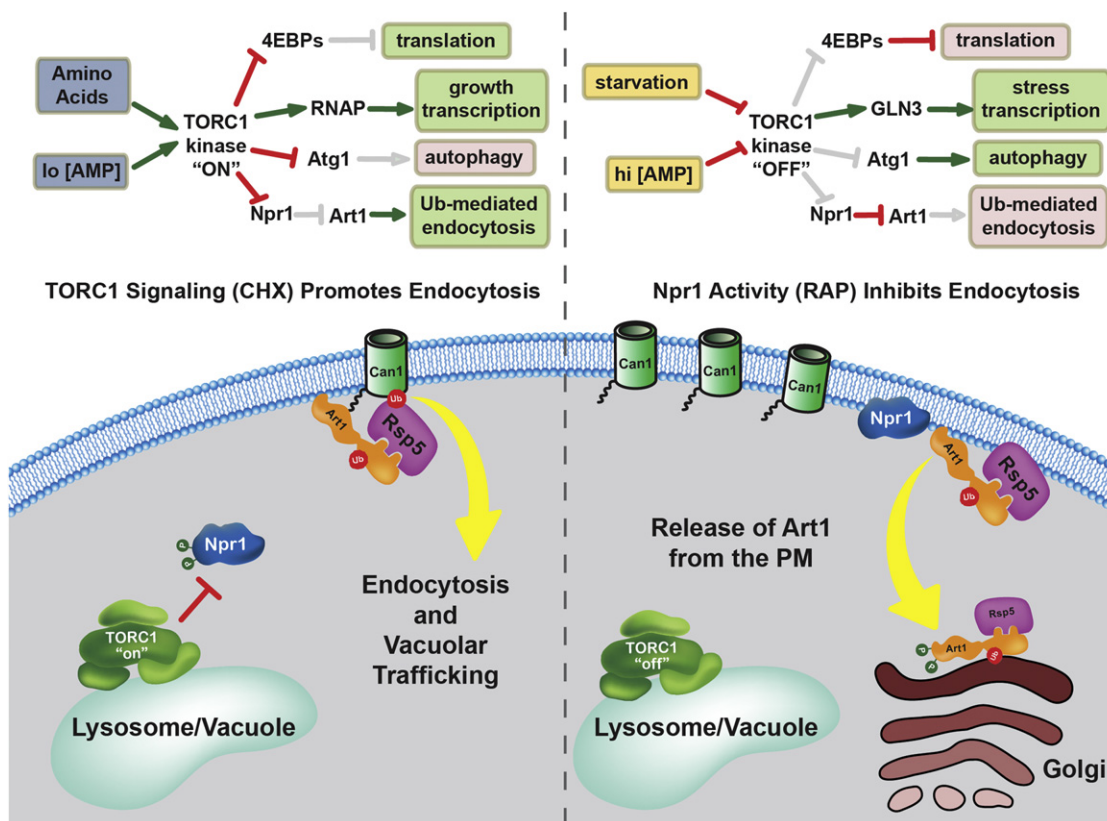


Figure 7. A Mechanism for TORC1 Regulation of Endocytosis

When TORC1 signaling is “on” (left panel), Npr1 is phosphoinhibited which promotes endocytosis of specific transporters by promoting Art1-Rsp5 translocation to the PM. When TORC1 signaling is “off” (right panel), as occurs during rapamycin treatment or starvation conditions, Npr1 is active and can phosphorylate Art1, an inhibited state that favors Golgi and cytosol localization. This novel effector mechanism allows TORC1 to modulate ubiquitin-mediated endocytosis and provides new insights into TORC1-mediated coordination of diverse cellular processes to achieve growth control (top diagrams). Gray arrows and bars indicate the release of a regulatory interaction due to upstream regulatory effects in the pathway. See also Figure S8.

these phosphorylation events regulate endocytosis remains to be elucidated, but it seems likely given that both Art2 and Art3 have been shown to function in the endocytosis of specific cargoes (Hatakeyama et al., 2010; Lin et al., 2008). Furthermore, it is conceivable that other signaling pathways may similarly affect PM protein composition by regulating the activity of other ART family proteins.

A parallel strategy in mammalian cells might involve the family of uncharacterized arrestin-domain-containing (ARRDC) proteins, which exhibit a domain structure similar to ART family proteins with N-terminal arrestin domains and C-terminal PY motifs. One mammalian ARRDC family protein, ARRDC3, was recently shown to associate with the Nedd4 ubiquitin ligase and mediate the endocytic downregulation of β 2-adrenergic receptor (Nabhan et al., 2010). It is tempting to speculate that mammalian ARRDC family proteins may be subject to regulation by mTORC1 signaling, thus providing an mTORC1 effector branch analogous to the one presented in this study. Interestingly, mammalian β -arrestins are subject to a regulatory cycle that involves phosphoinhibition and activation by dephosphorylation (Lin et al., 2002), however further study will be required to

determine the extent to which TORC1 signaling regulates the function of arrestin-related proteins in mammalian cells.

The Npr1 Kinase Links Nutrient Sensing to Endocytosis

Previous studies have suggested a role for Npr1 in the trafficking of amino acid transporters, however a consensus role for Npr1 has been elusive. For example, one study presents evidence that the Npr1 kinase promotes endocytosis of the tryptophan transporter TAT2 (Schmidt et al., 1998). In contrast, other studies have provided evidence that the Npr1 kinase functions to stabilize transporters at the plasma membrane (De Craene et al., 2001). Our analysis demonstrates that Npr1 stabilizes the arginine transporter Can1 at the plasma membrane by antagonizing the function of Art1. Interestingly, the phosphoproteomic data presented in this paper (Table 1) may actually reconcile the seemingly contradictory reports regarding the role of Npr1 with respect to endocytosis. For example, although our results demonstrate that Npr1 negatively regulates endocytosis via phosphoinhibition of Art1, we also found several candidate Npr1 substrates that were plasma membrane-localized nutrient transporters. This result, combined with our observation that

active Npr1 is recruited to the PM, suggests that Npr1 may phosphorylate both Art1 and transporters at the PM. The consequence of cargo phosphorylation is unclear but we speculate that this may either regulate transporter activity or promote endocytosis. Thus, a better understanding of Npr1-mediated phosphorylation of nutrient transporters at the PM may help to resolve some of the contradictory reports regarding the role of Npr1 as a regulator of endocytosis.

The Npr1 kinase represents an important mediator of TORC1 control of endocytosis in yeast, but the existence of an analogous pathway in mammalian cells is unclear. Although Npr1 has no obvious homolog in human cells, it is part of a large family of kinases that includes the glucose-sensing kinase Snf1, the yeast homolog of the mammalian AMP-activated kinase. We speculate that the family of AMPK/Snf1-related kinases in both yeast and mammals may have evolved as sensors of nutrient availability that regulate growth responses including endocytosis and membrane traffic. Consistent with our observation that part of this response may involve regulation of endocytosis, Snf1 was shown to phosphorylate the arrestin-related protein Art4 (Shinoda and Kikuchi, 2007) and related kinases Hal4 and Hal5 have been implicated in stabilizing potassium transporters at the plasma membrane by an unknown mechanism (Pérez-Valle et al., 2007). Although it remains to be seen if mTORC1 regulates endocytosis in mammalian cells, we speculate that such regulation could involve effectors which include AMPK/Snf1-related kinases.

Endocytosis as an Effector of TORC1-Mediated Growth Control

In the current study, we elucidate a mechanism by which TORC1 controls the abundance of the Can1 arginine transporter at the PM. Importantly, by regulating the abundance of amino acid transporters at the plasma membrane, TORC1 can finely tune amino acid influx in response to various cellular signals and environmental conditions. For example, the prototype mechanism described in this study affords the cell very fine control over intracellular arginine concentration: Can1 is stabilized at the PM during starvation conditions but Can1 endocytosis is activated when the cell is nutrient replete. Additional studies will be required to determine how signals upstream of TORC1 are integrated to control endocytosis, but canavanine and thialysine hypersensitivity phenotypes reported for *Δrheb1* yeast strains indicate that the signals are integrated upstream of Rheb (Urano et al., 2000). Furthermore, proteomic analysis of Npr1 indicates that it can interact not only with TORC1 but also with Snf1 (Breitkreutz et al., 2010), suggesting that Npr1 function may integrate several modes of regulation. Thus, although our results demonstrate that regulation of endocytosis is an important branch of the TORC1 response, future studies will be required to determine how signals upstream of TORC1 as well as orthogonal signals are integrated to mediate this endocytic downregulation response.

It is intriguing to consider how the regulation of endocytosis contributes to the adaptive growth strategies mediated by TORC1 signaling. Interestingly, recent work in mammalian cells has demonstrated that nutrient transporters at the cell surface that facilitate the influx of leucine are required for TORC1 activity

(Nicklin et al., 2009). Thus, it is possible that TORC1-mediated endocytosis of amino acid transporters provides an autoinhibitory feedback loop that limits TORC1 activation (Figure S8A), consistent with our analysis of TORC1 signaling during a YPD shift timecourse (Figures S8B and S8C). Furthermore, the ability of TORC1 to sense misfolded proteins and respond by activating endocytosis could promote the turnover of misfolded or damaged proteins at the PM. Additionally, the role of TORC1 signaling as both a positive regulator of endocytosis and a negative regulator of autophagy is intriguing. In such an inversely-coordinated system, dampened TORC1 signaling during starvation conditions simultaneously activates autophagy and inhibits endocytosis of the arginine transporter at the PM, both of which contribute to the availability of amino acids. TORC1 coordination of two distinct membrane trafficking pathways toward a cooperative outcome is an elegant example of how signaling networks can harness complex cellular processes to regulate cell growth.

EXPERIMENTAL PROCEDURES

Plasmids, Strains, and Yeast Plating Assays

All plasmids and yeast strains used in this study are listed in Table S1 and Table S2, respectively. Canavanine plating assays were performed as previously described (Lin et al., 2008). Briefly, yeast cultures grown overnight in YPD were normalized to 1 OD/ml, serially diluted and plated onto SCD plates using a pin-frogger. The following concentrations of canavanine were tested in each experiment: 0 μg/ml, 1.0 μg/ml, 2.0 μg/ml, and 4.0 μg/ml.

Microscopy

All microscopy was performed using an Olympus IX71 microscopy equipped with FITC and rhodamine filters. Deconvolution and image analysis was performed using Softwrx software (Applied Precision). For cargo trafficking assays, strains expressing chromosomally-tagged Vph1-mCherry were used to label the vacuolar membrane. In most experiments, cells were either mock-treated or treated with cycloheximide (CHX) (50 μg/ml) and/or rapamycin (RAP) (200 ng/ml) for 1.5 hr prior to imaging cells. Vacuolar trafficking of cargo was quantified by measuring fluorescence intensity of cargo signal (GFP) in the vacuole normalized to signal at the PM. For Art1-GFP and Npr1-GFP localization experiments, cells were stimulated with CHX, RAP, or both for 10 min prior to imaging. Art1 PM translocation was quantified as illustrated in Figure S7C.

Amino Acid Uptake Assays

To measure amino acid (arginine) uptake, yeast cells were grown to midlog phase in SCD media and then labeled by addition of 5 μCi [³H] arginine (Perkin Elmer). Samples were collected at indicated time points by addition of ice-cold stopping solution (20 mM Na₃, 20 mM NaF). Cells were pelleted, and the amount of [³H] arginine remaining in the supernatant was measured using a Beckman Coulter LS 6500 scintillation counter.

Npr1 In Vitro Kinase Assay

Recombinant Art1-6xHis-FLAG was incubated with yeast purified wild-type or kinase dead GST-Npr1 for 30 min at 30°C in kinase buffer (50 mM Tris [pH 7.5], 20 mM MgCl₂, 1 mM DTT, 25 μM [γ-³²P]-ATP [Perkin Elmer]). (See Supplemental Information for detailed protein purification protocols.) Subsequently, Art1-6xHis-FLAG was purified by incubating with M2 Flag beads for 1 hr at 4°C. Beads were washed in TBS (50 mM Tris [pH 7.5] and 150 mM NaCl) and eluted in elution buffer (TBS with 5 mg/ml 3X FLAG Peptide [Sigma-Aldrich]). Protein samples were resolved by SDS-PAGE. Gels were both subjected to western blot and dried for autoradiographing with Kodak BioMax MS film [Sigma-Aldrich]).

SILAC and Quantitative Mass Spectrometry

All quantitative mass spectrometry analysis was performed using SILAC labeling of yeast strains auxotrophic for lysine and arginine. Cells were grown

to midlog phase in the presence of either heavy or light isotopes (lysine and arginine) and affinity purification was performed as described in Supplemental Methods. Heavy and light purified samples were mixed and digested with 1 μ g of trypsin for 2 hr at 37°C. For phosphoproteomics experiments, phosphopeptides were purified using IMAC chromatography as previously described (Albuquerque et al., 2008). Purified peptides were dried, reconstituted in 0.1% trifluoroacetic acid, and analyzed by LC-MS/MS using an Orbitrap XL mass spectrometer. Database search and SILAC quantitation was performed using Sorcerer software.

SUPPLEMENTAL INFORMATION

Supplemental Information includes Extended Experimental Procedures, two tables, and eight figures and can be found with this article online at doi:10.1016/j.cell.2011.09.054.

ACKNOWLEDGMENTS

We thank M.N. Hall, R. Loewith, and J. Thorner for helpful advice and discussion. We also thank Patrice Ohouo and Sunil Adige for technical advice and assistance. We are grateful to E. MacGurn for assistance with graphic design, and to Shu-Bing Qian and W. Michael Henne for critical reading of the manuscript. We also thank members of the Emr lab for helpful discussions, especially Chris Stefan. J.A.M. is supported by a Fleming Research Fellowship. P.H. is supported by a fellowship from the Taiwanese Ministry of Education.

Received: March 21, 2011

Revised: July 27, 2011

Accepted: September 21, 2011

Published: November 23, 2011

REFERENCES

- Albuquerque, C., Smolka, M., Payne, S., Bafna, V., Eng, J., and Zhou, H. (2008). A multidimensional chromatography technology for in-depth phosphoproteome analysis. *Mol. Cell. Proteomics* 7, 1389–1396.
- Binda, M., Peli-Gulli, M.P., Bonfils, G., Panchaud, N., Urban, J., Sturgill, T.W., Loewith, R., and De Virgilio, C. (2009). The Vam6 GEF controls TORC1 by activating the EGO complex. *Mol. Cell* 35, 563–573.
- Bonenfant, D., Schmelzle, T., Jacinto, E., Crespo, J.L., Mini, T., Hall, M.N., and Jenoe, P. (2003). Quantitation of changes in protein phosphorylation: a simple method based on stable isotope labeling and mass spectrometry. *Proc. Natl. Acad. Sci. USA* 100, 880–885.
- Breitkreutz, A., Choi, H., Sharom, J., Boucher, L., Neduva, V., Larsen, B., Lin, Z., Breitkreutz, B., Stark, C., Liu, G., et al. (2010). A global protein kinase and phosphatase interaction network in yeast. *Science* 328, 1043–1046.
- De Craene, J., Soetens, O., and Andre, B. (2001). The Npr1 kinase controls biosynthetic and endocytic sorting of the yeast Gap1 permease. *J. Biol. Chem.* 276, 43939–43948.
- Gander, S., Bonenfant, D., Altermatt, P., Martin, D., Hauri, S., Moes, S., Hall, M., and Jenoe, P. (2008). Identification of the rapamycin-sensitive phosphorylation sites within the Ser/Thr-rich domain of the yeast Npr1 protein kinase. *Rapid Commun. Mass Spectrom.* 22, 3743–3753.
- Gander, S., Martin, D., Hauri, S., Moes, S., Poletto, G., Pagano, M., Marin, O., Meggio, F., and Jenoe, P. (2009). A modified KESTREL search reveals a basophilic substrate consensus for the *Saccharomyces cerevisiae* Npr1 protein kinase. *J. Proteome Res.* 8, 5305–5316.
- Hatakeyama, R., Kamiya, M., Takahara, T., and Maeda, T. (2010). Endocytosis of the aspartic acid/glutamic acid transporter Dip5 is triggered by substrate-dependent recruitment of the Rsp5 ubiquitin ligase via the arrestin-like protein Aly2. *Mol. Cell Biol.* 30, 5598–5607.
- Holz, M.K., Ballif, B.A., Gygi, S.P., and Blenis, J. (2005). mTOR and S6K1 mediate assembly of the translation preinitiation complex through dynamic protein interchange and ordered phosphorylation events. *Cell* 123, 569–580.
- Inoki, K., Li, Y., Zhu, T., Wu, J., and Guan, K.L. (2002). TSC2 is phosphorylated and inhibited by Akt and suppresses mTOR signalling. *Nat. Cell Biol.* 4, 648–657.
- Inoki, K., Zhu, T., and Guan, K.L. (2003). TSC2 mediates cellular energy response to control cell growth and survival. *Cell* 115, 577–590.
- Kamada, Y., Yoshino, K., Kondo, C., Kawamata, T., Oshiro, N., Yonezawa, K., and Ohsumi, Y. (2010). Tor directly controls the Atg1 kinase complex to regulate autophagy. *Mol. Cell Biol.* 30, 1049–1058.
- Lin, C., MacGurn, J., Chu, T., Stefan, C., and Emr, S. (2008). Arrestin-related ubiquitin-ligase adaptors regulate endocytosis and protein turnover at the cell surface. *Cell* 135, 714–725.
- Lin, F., Chen, W., Shenoy, S., Cong, M., Exum, S., and Lefkowitz, R. (2002). Phosphorylation of beta-arrestin2 regulates its function in internalization of beta(2)-adrenergic receptors. *Biochemistry* 41, 10692–10699.
- Manning, B.D., Tee, A.R., Logsdon, M.N., Blenis, J., and Cantley, L.C. (2002). Identification of the tuberous sclerosis complex-2 tumor suppressor gene product tuberin as a target of the phosphoinositide 3-kinase/akt pathway. *Mol. Cell* 10, 151–162.
- Miranda, M., and Sorkin, A. (2007). Regulation of receptors and transporters by ubiquitination: new insights into surprisingly similar mechanisms. *Mol. Interv.* 7, 157–167.
- Nabhan, J.F., Pan, H., and Lu, Q. (2010). Arrestin domain-containing protein 3 recruits the NEDD4 E3 ligase to mediate ubiquitination of the [beta]2-adrenergic receptor. *EMBO Rep.* 11, 605–611.
- Nicklin, P., Bergman, P., Zhang, B., Triantafellow, E., Wang, H., Nyfeler, B., Yang, H., Hild, M., Kung, C., Wilson, C., et al. (2009). Bidirectional transport of amino acids regulates mTOR and autophagy. *Cell* 136, 521–534.
- O'Donnell, A., Apffel, A., Gardner, R., and Cyert, M. (2010). Alpha-arrestins Aly1 and Aly2 regulate intracellular trafficking in response to nutrient signaling. *Mol. Biol. Cell* 21, 3552–3566.
- Pérez-Valle, J., Jenkins, H., Merchan, S., Montiel, V., Ramos, J., Sharma, S., Serrano, R., and Yenush, L. (2007). Key role for intracellular K⁺ and protein kinases Sat4/Hal4 and Hal5 in the plasma membrane stabilization of yeast nutrient transporters. *Mol. Cell Biol.* 27, 5725–5736.
- Qian, S.B., Zhang, X., Sun, J., Bennink, J.R., Yewdell, J.W., and Patterson, C. (2010). mTORC1 links protein quality and quantity control by sensing chaperone availability. *J. Biol. Chem.* 285, 27385–27395.
- Sancak, Y., Bar-Peled, L., Zoncu, R., Markhard, A.L., Nada, S., and Sabatini, D.M. (2010). Ragulator-Rag complex targets mTORC1 to the lysosomal surface and is necessary for its activation by amino acids. *Cell* 141, 290–303.
- Schmidt, A., Beck, T., Koller, A., Kunz, J., and Hall, M.N. (1998). The TOR nutrient signalling pathway phosphorylates NPR1 and inhibits turnover of the tryptophan permease. *EMBO J.* 17, 6924–6931.
- Shinoda, J., and Kikuchi, Y. (2007). Rod1, an arrestin-related protein, is phosphorylated by Snf1-kinase in *Saccharomyces cerevisiae*. *Biochem. Biophys. Res. Commun.* 364, 258–263.
- Urano, J., Tabancay, A.P., Yang, W., and Tamanoi, F. (2000). The *Saccharomyces cerevisiae* Rheb G-protein is involved in regulating canavanine resistance and arginine uptake. *J. Biol. Chem.* 275, 11198–11206.